

Stability Study of an Exothermic Biocatalytic Reaction and its Application in Bioprocess Systems

M.R. Mohd. Radzi and M.H. Uzir*

*School of Chemical Engineering, Engineering Campus, Universiti Sains Malaysia,
Seri Ampangan, 14300 Nibong Tebal, Seberang Perai, Penang, Malaysia*

**E-mail: chhekarl@eng.usm.my*

ABSTRACT

Biocatalytic reaction is a type of reaction which uses enzyme or whole-cell as a (bio)-catalyst to achieve a desired conversion, under controlled conditions in a bioreactor. Temperature produces opposed effects on enzyme activity and stability, and is therefore a key variable in any biocatalytic processes. An exothermic biocatalytic reaction, in a continuous-stirred-tank reactor (CSTR), was analyzed where dynamic equations (non-linear differential equations) could be derived from the Michaelis-Menten and Arrhenius equations, by performing mass and energy balances on the reactor. In this work, the effects of the different parameters such as dilution rate, proportional control constant and dimensionless total enzyme concentration, on the stability of the system, were studied. The stability of the reaction could be analyzed, based on the ODE (ordinary differential equation), solved using the numerical technique in MATLAB® and the analytical investigation using Mathematica.® The numerical analysis can be carried out by considering the phase-plane behaviour and bifurcation diagrams of the dynamic equations, while the analytical analysis using Mathematica® can be undertaken by evaluating the eigenvalues of the system. In order to model the operational stability of biocatalysts, modulation factors need to be considered so that a proper design of bioreactors can be done. Temperature, as a key variable in such bioprocess systems, can be conveniently optimized through the use of appropriate models.

Keywords: Biocatalytic reaction, dynamical analysis, bifurcation, phase-plane analysis, eigenvalues analysis

INTRODUCTION

Biocatalytic reactions, with either enzyme or whole-cell as the catalyst, have long been used to catalyse chemical synthesis in order to obtain fine chemicals with specific structures (Adrie and Patrick, 2000). Enzyme, as an active catalyst, initiates or modifies the rate of a chemical reaction, and accelerates the system without itself being affected. Accordingly, biocatalysts can be divided into cellular (whether growing, resting or non-living cells) and non-cellular (enzymes which have been removed from the cellular membrane) types. Ribozymes, abzymes and peptide mimics can also be considered as biocatalysts (Benkovic and Ballesteros, 1997).

Biocatalysts have been applied in areas such as pharmaceuticals, detergents, and food products. As a matter of fact, recent advances in genetic engineering have improved stabilisation and immobilisation techniques of enzyme as biocatalyst. A better understanding of the structure-function relationships has also attracted a number of chemists and engineers to apply such methods outside these traditional businesses. Biocatalysis differs from

Received: 18 June 2007

Accepted: 29 October 2008

*Corresponding Author

conventional processes, not only by featuring a different type of catalysts, it also constitutes a new base of technology. The raw materials of a biologically-based process is built on sugar, lignin, animal or plant waste and the product range of biotechnological processes which often encompass chiral molecules or biopolymers such as proteins, nucleic acids or carbohydrates. Biocatalysts, including isolated enzymes, micro-organisms, plants, and catalytic antibodies, offer benefits such as environmentally-friendly materials, stereoselectivity and regioselectivity, as well as new reactions beyond the traditional chemical synthesis.

The development of the new biocatalysts and improvements, in process design and engineering, has fuelled and heightened interest in biocatalysis. The main objective is to solve some critical industrial problems and create alternative synthetic routes. As these technological advances evolve, emerging markets for biocatalysts, such as fine chemicals, pharmaceuticals and consumer products will result in a significant growth.

Biocatalyst has gone a step forward and it is competing with the conventional chemical catalysts. Potential advantages of biocatalysts include high specificity, high activity under mild environmental conditions, and high turnover number. Their biodegradable nature and label, as a natural product, have also become very important assets (Polastro, 1989). Drawbacks are inherent to their complex molecular structure, making them costly to produce, and are intrinsically unstable as well.

Temperature produces opposed effects on the activity and stability of enzyme, and for this reason, it is therefore a key variable in any biocatalytic processes (Andres, 1999). In order to study the effect of temperature on the rate of an exothermic biocatalytic reaction, two factors need to be considered. The first is the influence of temperature on the reaction rate constant, and the second is the thermal denaturation of enzymes at elevated temperatures, which counteracts the enhancement in the rate constant at higher temperature. The temperature range, over which enzymes exhibit their activities, is rather limited. At temperatures above 100°C, a number of enzymes relatively show substantial activities, while near the freezing temperatures, the rates become very slow (Harvey and Douglas, 1996). The thermal deactivation of enzymes limits their useful lifetime in processing environments, and is thus of considerable importance in process design and development. The temperature range, over which thermal denaturation occurs, varies with the nature of the enzyme being considered.

High temperature induces irreversible deactivation of enzymes. It enables the thermodynamic parameters of enzyme to be determined and is used to study the mechanisms involved in the biochemical systems. For example, the effects of this factor on the stability of *Rhizomucor miehei* lipase have been investigated. The stability criterion used was the residual hydrolytic activity of the lipase. Experimental and theoretical parameters, obtained by linear regression analysis, were compared with the theoretical kinetics to validate the series-type inactivation model. Lipase obtained from *R. miehei* was deactivated by either thermal or pressure treatment (Noel and Combes, 2003). There are many types of enzyme involved in the exothermic biocatalytic reaction and some of the examples are shown in Table 1. The main objective of this work was to determine the optimum conditions and parameters, for which an exothermic biocatalytic reaction reached a stable state.

THE MICHAELIS-MENTEN MODEL

The standard Michaelis-Menten equation, based on one-substrate-one-product, is given below.

$$-r_s = \frac{k_s[E_t][S]}{[S] + K_m} \quad (1)$$

TABLE 1
Examples of exothermic biocatalyst

Biocatalyst	Temperature Range (°C)	Comments
<i>Sulfolobus</i>	60 - 80	Important geochemical agent in the production of sulphuric acid from sulphur in high temperature hydrothermal systems.
<i>Sulfolobus metallicus</i>	70 - 80	Catalyst in bioleaching of chalcopyrite at 70°C for microbial catalysis of ferrous ion oxidation.
β -glucosidase from <i>Sulfolobus solfataricus</i>	70 - 80	Catalyst in lactulose production from lactose and fructose hydrolysis.
<i>Candida antarctica</i> lipase B	30 - 60	Catalyst for the biocatalytic production of chiral secondary alcohols.

where [S] is the substrate concentration (mol dm^{-3}), $[E_t]$ is the total enzyme concentration (mol dm^{-3}), K_m represents Michaelis-Menten Constant (mol dm^{-3}), and $k_3' = k_3[W]$ is the rate constant (s^{-1}).

Let V_{max} represent the maximum rate of reaction, for a given total enzyme concentration, $[E_t]$. Hence,

$$V_{max} = k_3'[E_t] \quad (2)$$

From Eq. (1), the Michaelis-Menten equation can simply be rewritten as:

$$-r_s = \frac{V_{max}[S]}{[S] + K_m} \quad (3)$$

THE MODEL OF EXOTHERMIC REACTION

Considering the biocatalytic reaction in the CSTR, substrate A was converted into product B through an enzymatic reaction. Therefore, the reaction rate, based on the Michaelis-Menten equation derived previously (in respective to this particular biocatalytic reaction for the decomposing rate of substrate A) is given by:

$$r_A = \frac{k_3' C_A C_{Et}}{C_A + K_m} \quad (4)$$

where r_A represents the moles of substrate A decomposing per hour per cubic meter of reacting mixture, C_A shows the concentration of A in the reacting mixture, C_{Et} is the total enzyme concentration, and K_m represents the Michaelis-Menten constant. Applying the Arrhenius equation for the rate constant k_3' ,

$$k_3' = k_A e^{E/RT} \quad (5)$$

where k_A is the reaction velocity constant (s^{-1}), E is the activation energy (J/mole), R is the universal gas law constant = 8.314 J/mole K, and T is the absolute temperature, (K). Substituting Eq. (5) with Eq. (4), the reaction rate could therefore be rewritten as:

$$r_A = \frac{k_A e^{-E/RT} C_A C_{Et}}{C_A + K_m} \quad (6)$$

For further derivation of the dynamic model of an exothermic biocatalytic reaction, a general mass balance of substrate A and energy balance on the CSTR was carried out.

The General Mass Balance of Substrate A

A general balanced equation, around the reactor system for component A, could be simply written, as:

$$F_{A_o} - F_A - \int^V r_A dV = \frac{dN_A}{dt} \quad (7)$$

hence;

$$FC_{A_o} - FC_A - r_A V = \frac{VdC_A}{dt} \quad (8)$$

where F_{A_o} represents the inlet mole flow rate of A (moles A/s), F_A is the outlet mole flow rate of A (moles A/s), F is the feed rate of the mixture to the reactor (m^3/s) C_{A_o} , is the inlet concentration of A ($mole/m^3$), C_A represents the outlet concentration of (A, $mole/m^3$) and V is the volume of the mixture (m^3). Substituting Eq. (6) with Eq. (8) leads to:

$$FC_{A_o} - FC_A - \frac{k_A e^{-E/RT} C_A C_{Et}}{C_A + K_m} V = \frac{VdC_A}{dt} \quad (9)$$

Rearranging Eq. (9), gives;

$$\Rightarrow \frac{dC_A}{dt} = \frac{F}{V} [C_{A_o} - C_A] - \frac{k_A e^{-E/RT} C_A C_{Et}}{(C_A + K_m)} \quad (10)$$

The following assumptions were made in order to arrive at Eq. (10); these include (i) the density of the reacting mixture is constant, unaffected by the conversion of A to B, (ii) the feed and product rates F are equal and constant, (iii) volume, V of the reacting mixture is constant, (iv) perfect mixing occurs, so that C_A is the same in the reactor and product stream.

The Energy Balance on the CSTR

A general heat balance around a CSTR can be represented as:

$$F_p C_p T_o - F_p C_p T + r_A V (\Delta H) - Q(T) = \rho V C_p \frac{dT}{dt} \quad (11)$$

where T_0 is the temperature of the feed stream, T is the temperature in the reactor, C_p is the specific heat of reacting mixture and ΔH refers to the heat of the reaction.

Substituting Eq. (6) with Eq. (11) gives:

$$F\rho C_p T_0 - F\rho C_p T + \left[\frac{k_A e^{-E/RT} C_A C_{Et}}{C_A + K_m} \right] V(\Delta H) - Q(T) = \rho V C_p \frac{dT}{dt} \quad (12)$$

Rearranging Eq. (12) leads to:

$$\rho V C_p \frac{dT}{dt} = F\rho C_p T_0 - F\rho C_p T + \left[\frac{k_A e^{-E/RT} C_A C_{Et}}{C_A + K_m} \right] V(\Delta H) - Q(T) \quad (13)$$

$$\frac{dT}{dt} = \frac{F}{V} [T_0 - T] + \frac{k_A (\Delta H) e^{-E/RT} C_A C_{Et}}{\rho C_p [C_A + K_m]} - \frac{Q(T)}{\rho V C_p}$$

In arriving to Eq. (13), three important assumptions should be followed; (i) the specific heat of the reacting mixture remains constant and unaffected by the conversion of A to B, (ii) a perfect mixing is achieved such that the temperature of the reacting mixture and the product stream are the same, and (iii) the heat of the reaction ΔH is constant, which is independent of the temperature and composition.

For further analysis, the dimensionless variable for the dynamic equations of this exothermic biocatalytic reaction as obtained previously was defined.

Using Eq. (10) by defining some dimensionless variables:

$$\tau = \frac{Ft}{V} = Dt \qquad y = \frac{C_A}{C_{A0}} \qquad \alpha = \frac{C_{Et}}{C_A + K_m}$$

$\frac{F}{V}$ is the dilution rate, and D , which refers to the rate of which the existing medium in the reactor, is replaced by a fresh medium α .

Dividing both sides of Eq. (10) with (DC_{A0}) :

$$\begin{aligned} \frac{dC_A}{dt(DC_{A0})} &= \frac{D[C_{A0} - C_A]}{DC_{A0}} - \frac{k_A e^{-E/RT} C_A C_{Et}}{(C_A + K_m)DC_{A0}} \\ \Rightarrow \frac{dy}{d\tau} &= 1 - y - \frac{k_A \alpha y}{D} e^{-E/RT} \end{aligned} \quad (14)$$

From Eq. (13):

$$\frac{dT}{dt} = \frac{F}{V} [T_0 - T] + \frac{k_A (\Delta H) e^{-E/RT} C_A C_{Et}}{\rho C_p [C_A + K_m]} - \frac{Q(T)}{\rho V C_p}$$

Defining θ_0 and θ with;

$$\theta = \frac{\rho C_p T}{C_{Ao}(\Delta H)} \qquad \theta_0 = \frac{\rho C_p T_0}{C_{Ao}(\Delta H)}$$

Multiplying both sides of Eq. (13) with $\frac{V\rho C_p}{FC_{Ao}(\Delta H)}$

$$\begin{aligned} \frac{dT}{dt} \left[\frac{V\rho C_p}{FC_{Ao}(\Delta H)} \right] &= \frac{F}{V} [T_0 - T] \left[\frac{V\rho C_p}{FC_{Ao}(\Delta H)} \right] + \frac{k_A(\Delta H)e^{-E/RT} C_A C_{Et}}{\rho C_p [C_A + K_m]} \left[\frac{V\rho C_p}{FC_{Ao}(\Delta H)} \right] \\ &\qquad - \frac{Q(T)}{V\rho C_p} \left[\frac{V\rho C_p}{FC_{Ao}(\Delta H)} \right] \\ \Rightarrow \frac{d\theta}{d\tau} &= \theta_0 - \theta + \frac{k_A y \alpha}{D} e^{-E/RT} - \frac{Q(T)}{FC_{Ao}(\Delta H)} \end{aligned} \tag{15}$$

From the dimensionless equation, $\theta = \frac{\rho C_p T}{C_{Ao}(\Delta H)}$, upon rearranging, leads to;

$$T = \frac{\theta C_{Ao}(\Delta H)}{\rho C_p} \tag{16}$$

Substitute Eq. (16) into Eq. (14);

$$\begin{aligned} \frac{dy}{d\tau} &= 1 - y - \frac{k_A y \alpha}{D} e^{-\frac{E}{R \left[\frac{\theta C_{Ao}(\Delta H)}{\rho C_p} \right]}} \\ \Rightarrow \frac{dy}{d\tau} &= 1 - y - \frac{k_A y \alpha}{D} e^{-\left[\frac{E\rho C_p}{R\theta C_{Ao}(\Delta H)} \right]} \end{aligned} \tag{17}$$

and similarly, Eq. (16) into Eq. (15) gives:

$$\frac{d\theta}{d\tau} = \theta_0 - \theta + \frac{k_A y \alpha}{D} e^{-\left[\frac{E\rho C_p}{R\theta C_{Ao}(\Delta H)} \right]} - \frac{Q(T)}{FC_{Ao}(\Delta H)} \tag{18}$$

Eq. (17) and Eq. (18) then become:

$$\left. \begin{aligned} \frac{dy}{d\tau} &= 1 - y - r(y, \theta) \\ \frac{d\theta}{d\tau} &= \theta_0 - \theta + r(y, \theta) - q(\theta) \end{aligned} \right\} \tag{19}$$

$$r(y, \theta) = \frac{k_A y \alpha}{D} e^{-\left[\frac{E \rho C_p}{R C_{Ao} (\Delta H)}\right]}$$

where;

$$q(\theta) = \frac{Q(T)}{F C_{Ao} (\Delta H)}$$

Based on the famous work by Aris and Amundson (1958), a form of control heat-removal function $q(\theta)$ was chosen and it is given by:

$$q(\theta) = U(\theta - \theta_c) [1 + K_c (\theta - \theta_s)] \tag{20}$$

where θ_c is the dimensionless mean temperature of water in the cooling coil which indicates that the heat removal is always proportional to the difference between the reactor temperature and the mean cooling-water temperature.

The term in brackets indicates that the proportional control on the cooling-water flow rate is present. The flow rate is increased by an amount proportional to the difference between the actual reactor temperature, θ and the desired steady-state temperature, θ_s , with K_c as the proportional control constant. The increase in the rate of the cooling-water flow is assumed for convenience to cause an approximately proportional increase in the heat removal. The constant U is a dimensionless analogue of $U_o A$, the overall heat-transfer rate. Defining $\beta = \frac{E \rho C_p}{R C_{Ao} (\Delta H)}$ and substituting Eq. (20) with Eq. (19), the final

dynamic equation to be studied is:

$$\left. \begin{aligned} \frac{dy}{d\tau} &= 1 - y - \frac{k_A y \alpha}{D} e^{-\frac{\beta}{\theta}} \\ \frac{d\theta}{d\tau} &= \theta_0 - \theta + \frac{k_A y \alpha}{D} e^{-\frac{\beta}{\theta}} - U(\theta - \theta_c) [1 + K_c (\theta - \theta_s)] \end{aligned} \right\} \tag{21}$$

RESULTS AND DISCUSSION

The Effect on Varying the Dilution Rate, D

The dilution rate D was the first parameter considered in this work; it refers to the rate of which the existing medium in the reactor is replaced by a fresh medium. The system was analyzed at three different values of K_c , by varying the values of the dilution rate. The difference between the stability of each system could then be analyzed.

Fig. 1 was numerically solved using the MATLAB® by applying ODE23 at a constant proportional control constant, $K_c = 10$, and varying the value of the dilution rate D , from 20 s^{-1} to 90 s^{-1} . This simulation was undertaken in order to study the effect of the increasing values of D on the stability of the system. *Fig. 4* shows that for the system with $K_c = 10$, the trajectory from the numerical integration resulted in a spiral focus for each value of D , but changing in the focus point. The non-formation of Hopf bifurcations resulted in no limit

cycle in this system. Increasing the value of D at $K_C=10$ would result in the decrease of the dimensionless temperature θ values, while reactant A conversion y was found to increase from 0 to 1. A further analysis was undertaken using the MATLAB® to study this dynamical system, as shown in *Figs. 2 (a) and (b)*. Plotting y against D and θ against D respectively shows that θ is decreasing while y is increasing with the increment in D , and stable focus without any bifurcation behaviours. This system can easily be maintained and controlled.

Meanwhile, increasing the dilution rate would result in a higher amount of substrate added into the reactor; therefore increasing the rate of the substrate diffusion into the active sites of enzyme to initiate the reaction. The diffusion of the substrate and product, inside a porous biocatalyst, was found to occur in parallel with the catalyzed reaction. The more enzyme catalyses the reaction reduced the substrate concentration within the particles, the greater the substrate concentration gradient created between the internal microenvironment and the bulk of the solution would be. In turn, this would increase the rate, at which the substrate was delivered to the enzyme molecules towards the outside of the particles, and increase y . However, there was a decrease in θ as the dilution rate D increased from 20 s^{-1} to 90 s^{-1} . As there was a constant amount of cell in the reactor, the active sites of the enzyme would fully be utilised by the substrate. Increasing the dilution rate caused the heat (released by the reaction) to be dissipated on the excess amount of the substrate and at the same time, lowered the temperature of the reactor.

The analysis was carried out mainly to look at the effect of increasing the value of D on the stability of the system at $K_C = 9$. The numerical integration, using the MATLAB® from the model equations, was plotted in *Fig. 3*, indicating that the system varied in the value of the dilution rate D , i.e. from 10 s^{-1} to 80 s^{-1} . Trajectories (in the form of stable spiral focus) appeared for D , which was equal to 10 s^{-1} , 20 s^{-1} , 30 s^{-1} and 40 s^{-1} . Limit cycles were formed when the values of D were 50 s^{-1} and 60 s^{-1} . Any further increase in D would result in stable focus points with a better stability.

In addition, further analysis of this dynamical system was undertaken, based on the stability diagram of the model equations at $K_C = 9$, as shown in *Figs. 4 (a) and (b)*. It is obvious that there were Hopf bifurcations (which appeared in between the two Hopf points) in

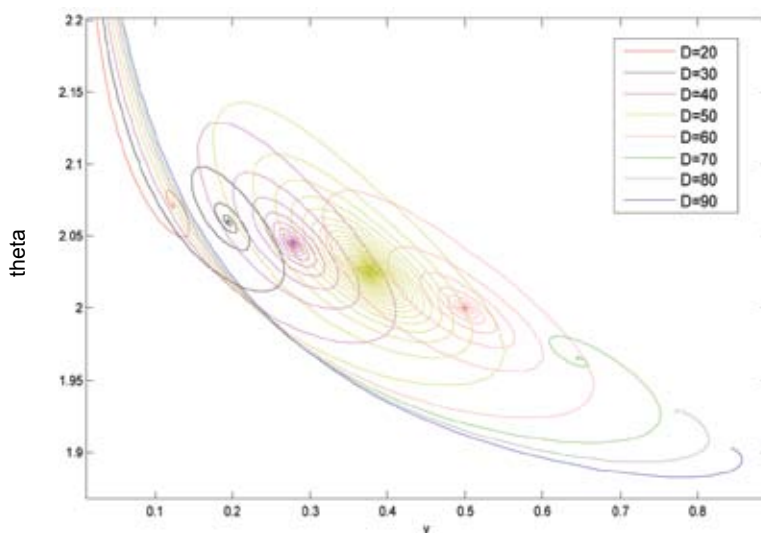


Fig. 1: Phase-plane of model equations at $K_C = 10$ at various dilution rates, D

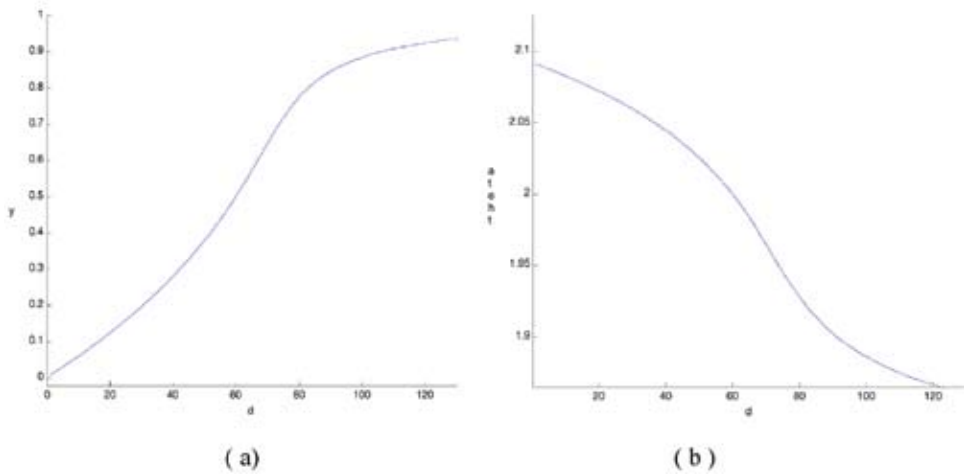


Fig. 2: Stability diagram of model equations at $K_c = 10$ with no bifurcations: (a) Bifurcation diagram y versus D and (b) Bifurcation diagram θ versus D

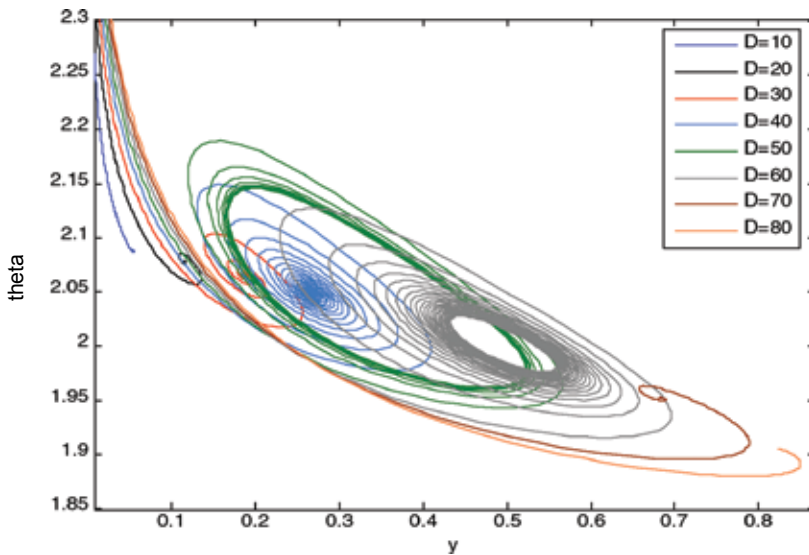


Fig. 3: Phase-plane of model equations at $K_c = 9$ at various dilution rates, D

this system. The first Hopf point was at $y = 0.2914$, $\theta = 2.0448$ and $D = 42.6748$, while the second Hopf point was at $y = 0.5$, $\theta = 2.0$ and $D = 60.00$. These bifurcations occurred when there were changes in the stability of the system, i.e. from the stable node or spiral focus to the limit cycles and vice versa. Bifurcation was observed in this system because there was instability in the enzyme, under this range of conditions.

The same analysis was repeated for the purpose of studying the effect of increasing the value of D on the stability of the system at $K_c = 7$. Fig. 5 shows the phase-plane of θ versus, y , at a proportional control constant, $K_c = 7$ with variable dilution rates D , from 20 s^{-1} to 80 s^{-1} . This system resulted in a stable spiral focus for D , which equalled to 20 s^{-1} and 30 s^{-1} .

The limit cycles were formed when the values of D varied at 40 s^{-1} , 50 s^{-1} and 60 s^{-1} . If the dilution rate D increased further, the limit cycles would disappear and a good control could be achieved.

Further analysis of this dynamical system was carried numerically, as shown in *Figs. 6 (a) and (b)*. Again, the Hopf bifurcations were observed to occur in between the two Hopf points. The first Hopf point was at $y = 0.2270$, $\theta = 2.0649$ and $D = 38.6688$, while the second Hopf point was at $y = 0.6271$, $\theta = 1.9636$ and $D = 63.5063$. These bifurcations evolved when there were changes in the stability of the system, i.e. from spiral focus to limit cycles and vice versa.

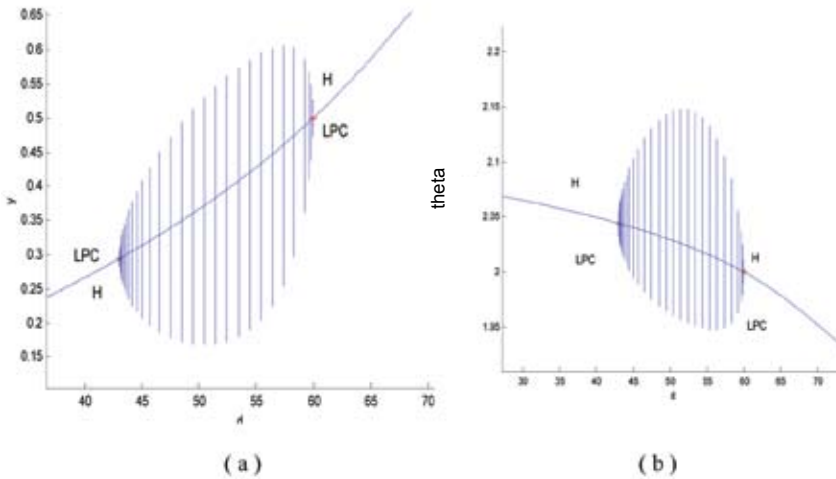


Fig. 4: Bifurcation diagram of model equations at $K_c = 9$: (a) plot y versus D and (b) plot θ versus D

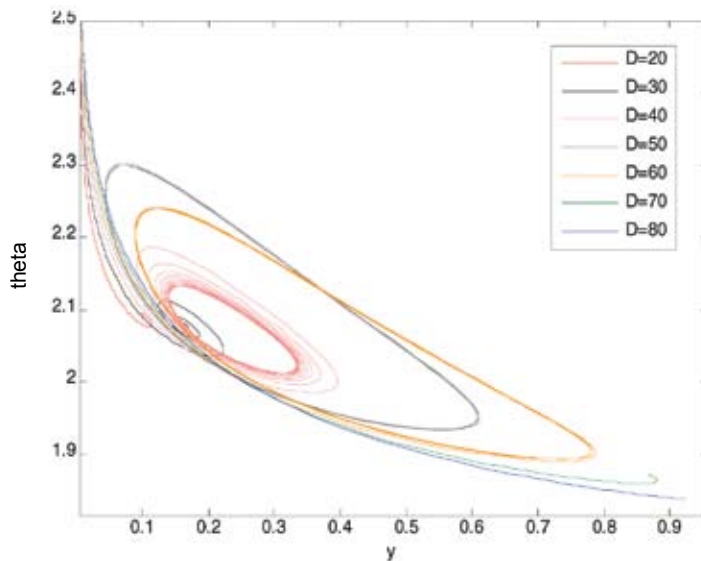


Fig. 5: Phase-plane of model equations at $K_c = 7$ at various dilution rates, D

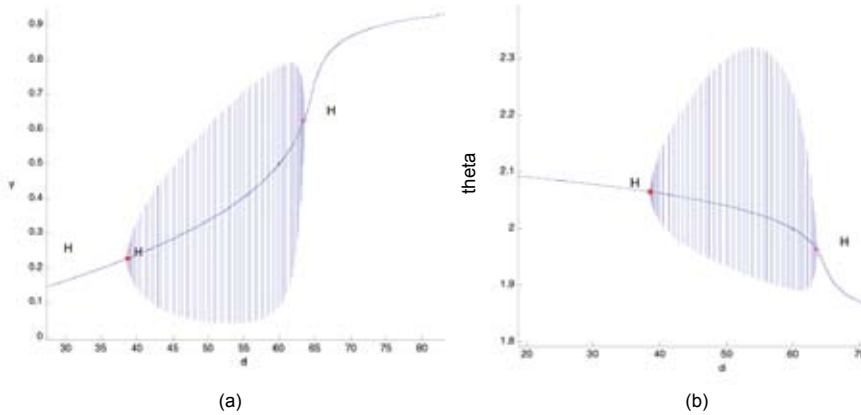


Fig. 6: Bifurcation diagram of model equations at $K_c = 7$: (a) plot y versus D and (b) plot θ versus D

The Effect of Changes in the Proportional Control Constant, K_c

The second parameter being considered was the proportional control constant, K_c which referred to the proportional control of the cooling-water flow rate. Such an increase in cooling water flow rate was assumed for convenience, i.e. to obtain an approximate proportional increase in heat removal (Donald, 1991). For this purpose, the system was analysed, at three different values of D , by varying the value of K_c . The difference between the stability of each system could then be analyzed. Taking an example of the system at $D = 50$, the results from the simulation are shown in Figs. 7 and 8.

Referring to the above figures, the stability of the system was analyzed at the dilution rate, D which was equal to $50s^{-1}$ and varied in the value of proportional control constant, K_c . This system resulted in a stable spiral focus for $K_c = 1$. Limit cycles were then formed when $K_c = 2$. As a result, a stable steady-state, formed for K_c , was equal to 3 and 4. Limit cycles

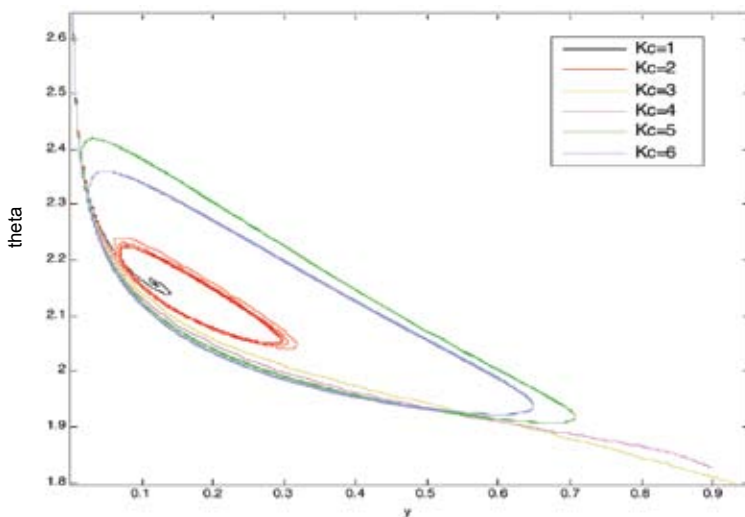


Fig. 7: Phase-plane of model equations at $D = 50$ at various K_c (1-6)

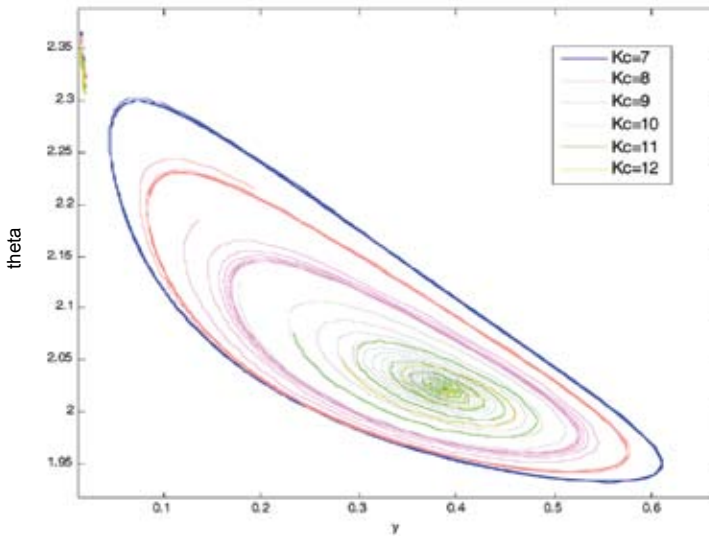


Fig. 8: Phase-plane of model equations at $D = 50$ at various K_c (7-12)

then appeared when the values of K_c varied from 5 to 9. Further increase in the value of K_c would result in a stable spiral focus. If the dilution rate D was increased further, the limit cycles would disappear and a stable reaction system could be achieved.

To make the observation easier, the bifurcation diagrams were plotted as shown in *Figs. 9, 10 and 11*, i.e. at three different values of D . According to the analysis carried out, and based on the phase-plane of the model equations in *Figs. 9, 11 and 13*, the dimensionless temperature of the reactor θ was found to decrease with the increase in the proportional control constant K_c . Meanwhile, the reactant conversion y increased with the increase in K_c . The limit cycles were also observed to appear in each system.

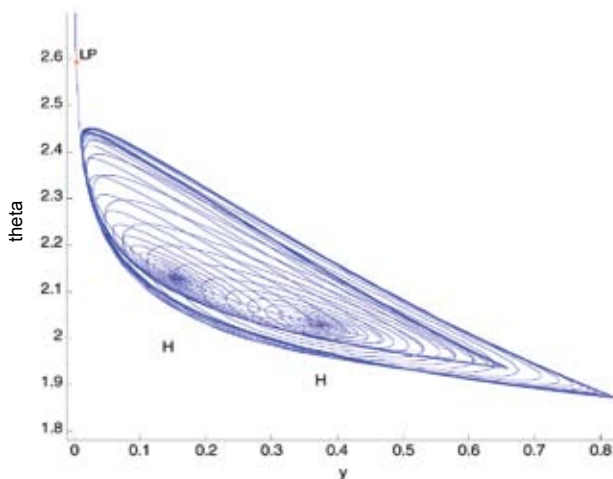


Fig. 9: Phase-plane of model equations at $D = 50$ at various K_c

From the bifurcation diagrams, it can be concluded that the types of bifurcation formed are different from one another. Based on the data presented in *Fig. 10*, there are Hopf bifurcations which appeared in between the two Hopf points, at $D = 50$. The first Hopf point was at $y = 0.1563$, $\theta = 2.1280$ and $K_c = 1.812$, while the second Hopf point was at $y = 0.3746$, $\theta = 2.0268$ and $K_c = 9.6945$. However, there is a region of stable steady-state in between this range of bifurcation. Referring to *Fig. 12* for system at $D = 60$, there is a small Hopf bifurcation which was formed at a Hopf point $y = 0.1483$, $\theta = 2.1504$ and $K_c = 0.847$. As for the third system analyzed at $D = 40$, the Hopf bifurcation re-appeared in between the two Hopf points. The first Hopf point was indicated at $y = 0.1823$, $\theta = 2.0916$ and $K_c = 4.2924$, while the second Hopf point was at $y = 0.2537$, $\theta = 2.0554$ and $K_c = 8.0131$.

As discussed in the earlier section, K_c refers to the proportional control on the cooling-water flow rate. The increase in the cooling water flow rate would cause an approximately proportional increase in the heat removal. Therefore, the amount of heat removed from

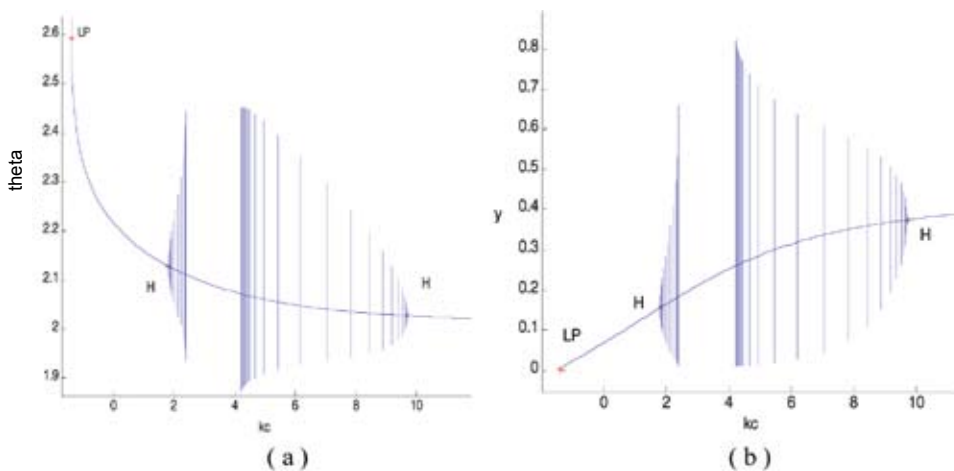


Fig. 10: Bifurcation diagram of model equations at $D = 50$; (a) plot θ versus K_c and (b) plot y versus K_c

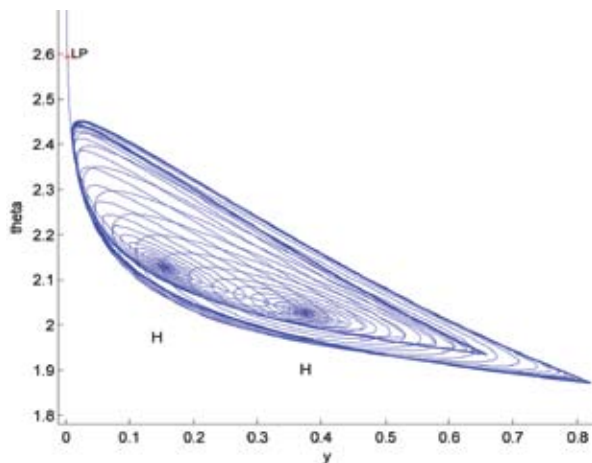


Fig. 11: Phase-plane of model equations at $D = 60$ at various K_c

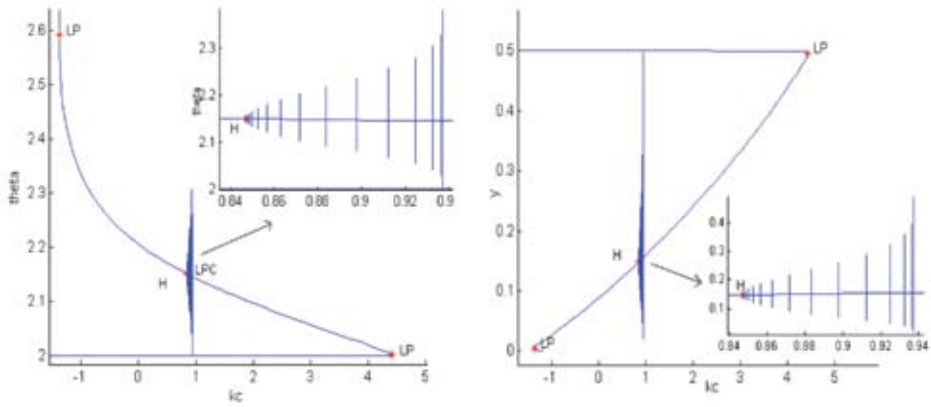


Fig. 12: Bifurcation diagram of model equations at $D = 60$; (a) plot θ versus K_C and (b) plot y versus K_C

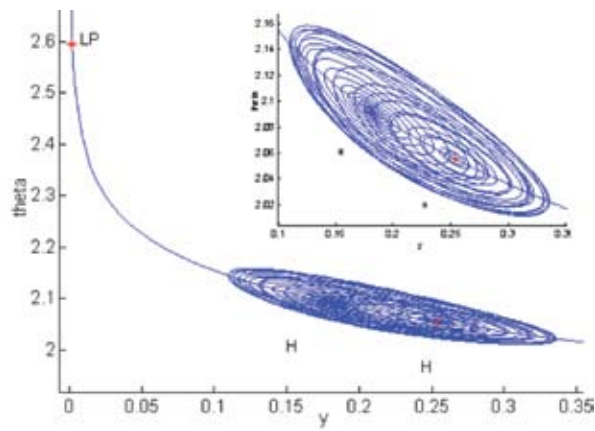


Fig. 13: Phase-plane of model equations at $D = 40$ at various K_C

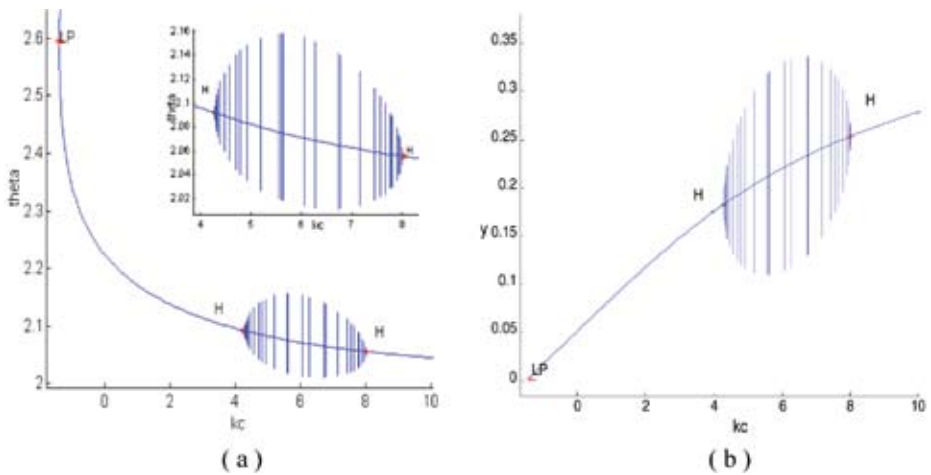


Fig. 14: Bifurcation diagram of model equations at $D = 40$; (a) plot θ versus K_C and (b) plot y versus K_C

the system was higher at higher values of K_C , the condition which would lower the reactor temperature. The increase in K_C resulted in the increase in the reactant conversion, as the heat removal from the system provided a suitable or an optimum temperature for the enzyme to have an optimum activity. This optimum operating condition would therefore promote more substrate to diffuse into active site of the enzyme, which further later led to substrate conversion.

At a lower value of K_C , the reactant conversion was found to be very low because the amount of heat removed was low, and this caused the temperature of the system to increase. As a result, the internal energy of the molecules in the system would also increase. The internal energy of the molecules might include the translational energy, vibrational energy and rotational energy, the energy involved in the chemical bonding of molecules as well as the energy involved in the non-bonding interactions. Some of this heat might be converted into a chemical potential energy. If this chemical potential energy increase was great enough, some of the weak bonds which determined the three dimensional shape of the active proteins might be broken. This could lead to a protein thermal denaturation and thus inactivate the enzyme. Therefore, too much of heat could also cause the rate of an enzyme-catalysed reaction to decrease, as the enzyme became denatured and inactive (Bommarius, 2004).

The effect on changes in the total enzyme concentration, α

The third parameter to be considered is the dimensionless total enzyme concentration, α which refers to the total amount of cells or enzyme in the reactor. Here, the system was analyzed at constant value of $D = 50$ and $K_C = 10$ with variable values of α .

From the phase-plane plotted in *Fig.15*, it could be observed that there were no bifurcations occurred in the system; this resulted in the non formation of the limit cycles. The increase in the total cell concentration α was found to increase the reactant conversion y , since there were more cells to react with the substrate added to the reactor. Meanwhile, the increase in the reactor temperature was basically due to the increase in the metabolic rate of the cell during the growth phase. The nutrient consumed was becoming less since the cell was at a stage of reproducing new cells. For α higher than 40, oscillations started to emerge in the system before it reached the equilibrium point, due to the interaction of cell with the high temperature. The enzyme was also found to be unstable, at a certain high temperature, even when the amount of cells was relatively high.

The Effect of Different Initial Conditions

The objective of this section was to study the effect of changing the values of the

dimensionless initial point $y = \frac{C_A}{C_{A_0}}$ and $\theta = \frac{\rho C_p T}{C_{A_0}(\Delta H)}$, which represented the conversion

reactant A and the dimensionless reactor temperature on the stability of reaction. Phase-plane was plotted using MATLAB® for two different systems, with graphically different initial points.

Figs. 16 and 17 show that the phase-plane portrait for the system at $D = 50 \text{ s}^{-1}$ and $K_C = 8$ resulted in a stable limit cycle, while the spiral focus appeared for the second system. For both systems, it could be clearly seen that varying the initial values did not impose any effect on the stability of the reaction, and this was followed by the same loops of stability which moved towards the same equilibrium point.

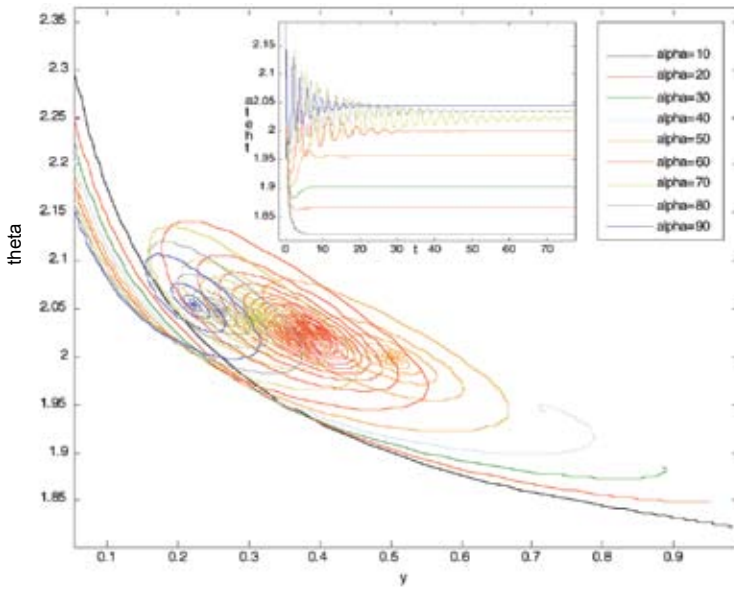


Fig. 15: Phase-plane of model equations at $K_c = 10$ and $D = 50$ at various α

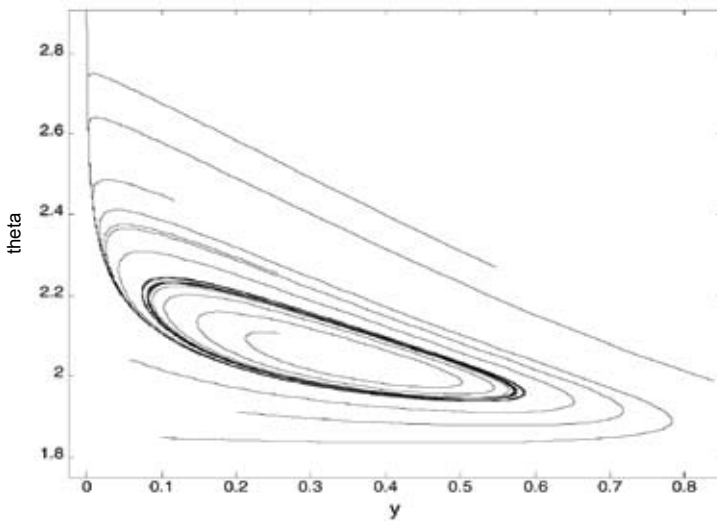


Fig. 16: Phase-plane portrait for system at $D = 50 \text{ s}^{-1}$ and $K_c = 8$ with changes in the initial points

The Analytical Investigation on the Thermal Stability of Biocatalytic Reaction

The results discussed previously involved the transition of the reaction stability (from the stable steady-state point and stable focus) to the formation of the limit cycles which could be proven mathematically using the eigenvalue analysis. Such an analysis was carried out using Mathematica® on two dynamic equations. Taking an example of the system at $K_c = 7$ and varying the value of D , the results gathered for the stability of the system could be simplified as in the Table 2 and Fig. 20.

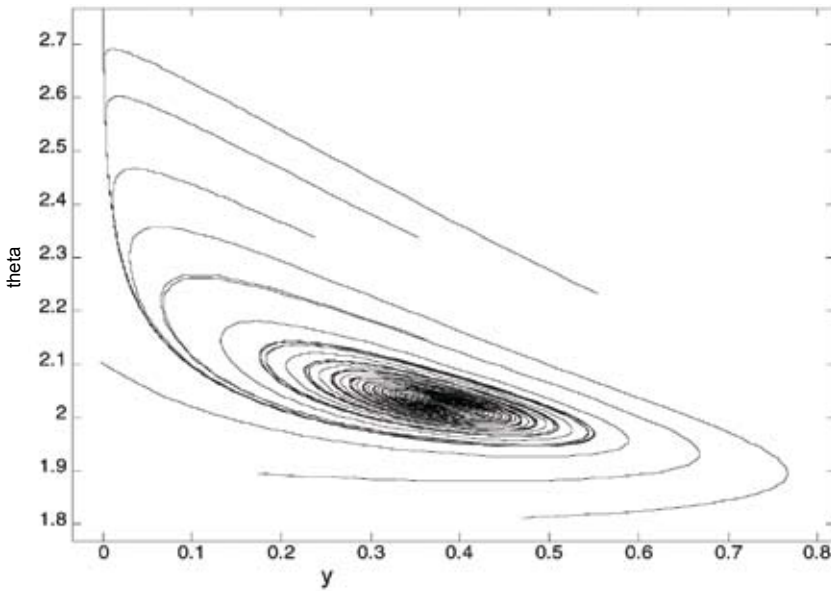


Fig. 17: Phase-plane portrait for system at $D = 50 \text{ s}^{-1}$ and $K_c = 10$ with changes in the initial points

TABLE 2
Equilibrium point coordinates and eigenvalues for system at $K_c = 7$

D (s^{-1})	Equilibrium Coordinates		Eigenvalues
	y	θ	
5	0.02310	2.10614	-10.4368 -7.0869
20	0.10101	2.09095	-2.3210 + 5.8362i -2.3210 - 5.8362i
30	0.16300	2.07839	-0.6471 + 4.4308i -0.6471 - 4.4308i
40	0.23800	2.06256	0.0642 + 3.2368i 0.0642 - 3.2368i
50	0.33655	2.04052	0.3392 + 2.1786i 0.3392 - 2.1786i
60	0.50010	1.99997	0.2498 + 1.0892i 0.2498 - 1.0892i
70	0.86795	1.87065	-0.7262 -0.4782
80	0.92288	1.83861	-0.9148 -0.5187

Based on the data presented in the table, changes were observed in the equilibrium points of this system for the different values of dilution rates D , which ranged from 5 s^{-1} to 80 s^{-1} . The dimensionless conversion y was found to increase with an increment in D , which was due to the addition of the substrate into the reactor. This had also increased the opportunity of substrate diffusion into the active sites of the enzyme to initiate the reaction. However,

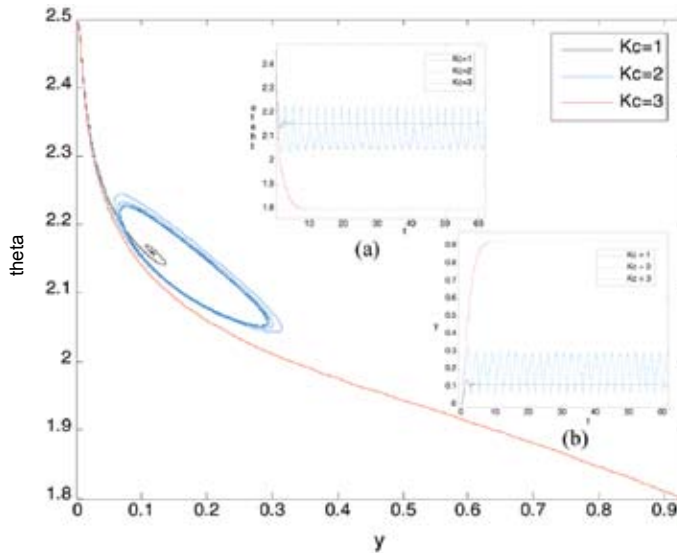


Fig. 18: Phase-plane portrait for system at $D = 50 \text{ s}^{-1}$ with varying proportional constant, K_C : (a) Plot θ versus t and (b) Plot y versus t

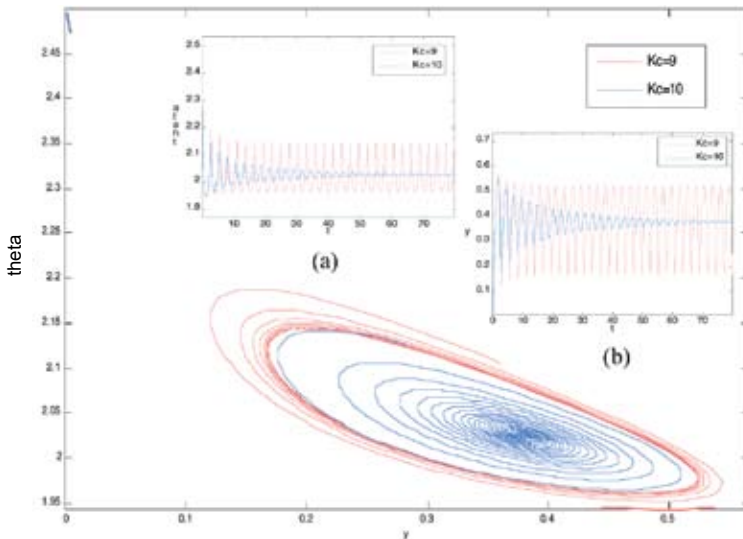


Fig. 19: Phase-plane portrait for system at $D = 50 \text{ s}^{-1}$ with varying proportional constant, K_C : (a) Plot θ versus t and (b) Plot y versus t

the values of the dimensionless temperature of the reactor were also found to decrease, as D increased from 5 s^{-1} to 80 s^{-1} . As there was a constant amount of enzyme in the reactor, the active sites of the enzyme would be fully utilized by the substrate. Increasing the dilution rate had caused the heat to release by the reaction to be dissipated on the excess amount of substrate and at the same time lowering the temperature of the reactor.

The eigenvalues obtained from the analysis were plotted in order to study the transition of the stability in the system (Fig. 20). From the figure, it can be observed that for $D = 5 \text{ s}^{-1}$, there was a stable node and for $D = 20 \text{ s}^{-1}$ there was a stable spiral focus. For the system with $D = 50 \text{ s}^{-1}$, the eigenvalues were found to be positive in the real part which was located in the unstable region with the formation of limit cycle. Therefore, there were transition points, from the stable region to the unstable region, in between $D = 20 \text{ s}^{-1}$ and $D = 50 \text{ s}^{-1}$. The Hopf bifurcations were found to occur when a conjugated complex pair crossed the boundary of the stable region.

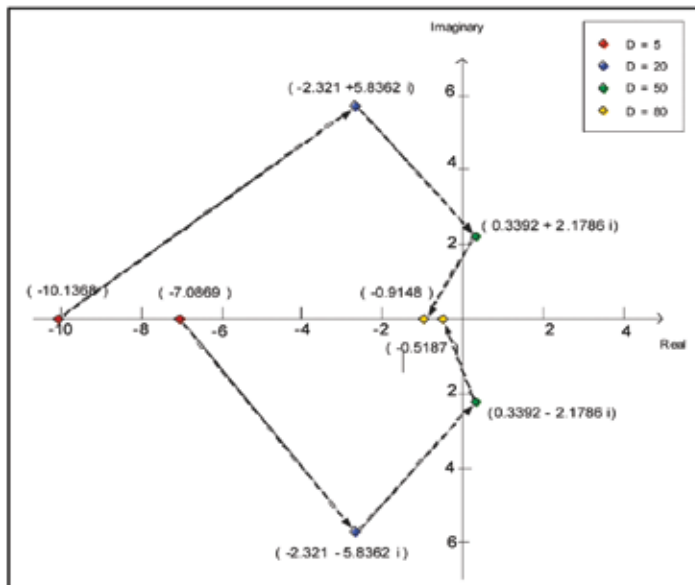


Fig. 20: Transition of stable point to limit cycle analyzed on system at $K_c = 7$

CONCLUSIONS

The evaluation of the model was discussed using both the graphical measures and mathematical analysis. Based on the observation of the graphs and discussions, some conclusions can therefore be put together. Modelling the operational stability of biocatalysts and considering modulation factors are required for a proper design of bioreactors. Temperature, as the key variable in such a bioprocess system, could be conveniently optimized through the use of appropriate models.

Three parameters were analyzed in this project; these were dilution rate (D), the proportional control constant (K_c) and the dimensionless total enzyme concentration (α). Each parameter discussed could have a different effect on the stability of the system, especially on the variables to be controlled in the dynamic equation, such as the dimensionless reactor

temperature (θ) and the dimensionless conversion of reactant (y). In some cases studied in this research, some Hopf bifurcations were formed in the phase-plane plot, indicating that there was a transformation in the stability loop from the stable node or spiral focus into limit cycle. The existence of the Hopf bifurcations had been successfully proven using the numerical technique and the eigenvalues analysis.

A study on the stability of such an exothermic biocatalytic reaction is very important as its results can be applied in the controlling process systems in optimum and stable conditions.

REFERENCES

- ADRIE J.J. STRAATHOF and ADLERCREUTZ, P. (2000). *Applied Biocatalysis*, 2nd ed., Harwood Academic Publishers.
- ANDRÉS I. (1999). Stability of biocatalysts. *Electronic Journal of Biotechnology*, 2(1).
- BENKOVIC, S. and BALLESTEROS, A. (1997). Biocatalysts-the next generation. *Trends in Biotechnology*, 15, 385-386.
- BRIGGS, G.E. and HALDANE, J.B. (1925). A note on the kinetics of enzyme action. *Biochem J.* 19(2), 338-9.
- BOMMARIUS, A.S and RIEBEL, B.R. (2004). *Biocatalyst: Fundamentals and Applications*. Wiley-VCH.
- OURIQUE, C.O., EVARISTO, C.B. and JOSE, C.P. (2002). The use of particle swarm optimization for dynamical analysis in chemical processes. *Computers and Chemical Engineering*, 26, 1783-1793.
- KAPLAN, D. and GLASS, L. (1995). *Understanding Nonlinear Dynamics*. New York: Springer.
- DONALD, R. and COUGHANOWR, R. (1991). *Process Systems Analysis and Control* (2nd Edition). New York: McGraw-Hill.
- BLANCH, H.W. and CLARK, D.S. (1996). *Biochemical Engineering*. U.S.A: Marcel Dekker Inc, U.S.A.
- HENLEY, J. and SADANA, A. (1986). Deactivation theory. *Biotechnology and Bioengineering*, 28, 1277-1285.
- GIBBS, P.R., UEHARA, C.S., NEUNERT, U. and BOMMARIUS, A.S. (2005). Accelerated biocatalyst stability testing for process optimization. *Biotechnol Prog* May-Jun, 21(3), 762-74.
- KOSHLAND D.E. (1958). Application of a theory of enzyme specificity to protein synthesis. *Proc. Natl. Acad. Sci.* Feb; 44(2), 98-104. U.S.A.
- LUCIA RUSSO and C.SILVESTRO. Nonlinear analysis of a network of three continuous stirred tank reactors with periodic feed switching: Symmetry and symmetry-breaking. *Int. J Bifurcation and Chaos*, 14, 1325-1341.
- NOEL M. and D. COMBES. (2003). Effects of temperature and pressure on *Rhizomucor miehei* lipase stability. *Journal of Biotechnology*, 23-32.
- PEREZ M., FONT R. and MONTAVA M.A. (2002). Regular self-oscillating and chaotic dynamics of a continuous stirred tank reactor. *Computers and Chemical Engineering*, 26, 889 – 901.
- PARKER H. (2005). Accelerated biocatalyst stability testing for process optimization. *Biotechnol Prog.*, 21(3), 762-74.
- PETER B. KAHN and YAIR ZARMI. (1998). *Nonlinear Dynamics: Exploration through Normal Forms*. Wiley.

- POLASTRO, E. (1989). Enzymes in the fine-chemicals industry: dreams and realities. *Bio/Technology* 7, 1238-1241.
- SEBORG D.E., EDGAR THOMAS F and MELLICAMP, DUNCAN A. (2004). *Process Dynamic and Control*. (2nd Edition). Wiley-VCH.
- YEONG S.K., CHANG S.P. and DEOK K. (2006). Lactulose production from lactose and fructose by a thermostable β -galactosidase from *Sulfolobus solfataricus*. *Enzyme and Microbial Technology*, 39, (4),903-908.